Inverse cascade in decaying three-dimensional magnetohydrodynamic turbulence

Mattias Christensson* and Mark Hindmarsh†
Centre for Theoretical Physics, University of Sussex, Brighton BN1 9QJ, United Kingdom

Axel Brandenburg‡
Nordita, Blegdamsvej 17, DK-2100 Copenhagen, Denmark
and Department of Mathematics, University of Newcastle, Newcastle upon Tyne NE1 7RU, United Kingdom
(Received 22 November 2000; published 22 October 2001)

We perform direct numerical simulations of three-dimensional freely decaying magnetohydrodynamic turbulence. For helical magnetic fields, an inverse cascade effect is observed in which power is transfered from smaller scales to larger scales. The magnetic field reaches a scaling regime with self-similar evolution, and power-law behavior at high wave numbers. We also find power-law decay in the magnetic and kinematic energies, and power-law growth in the characteristic length scale of the magnetic field.

DOI: 10.1103/PhysRevE.64.056405 PACS number(s): 95.30.Qd, 47.65.+a, 47.40.−x, 98.80.−k

I. INTRODUCTION

Within cosmology, astrophysics, or geophysics one often needs to deal with electrically conducting plasmas at high kinematic and magnetic Reynolds numbers where magnetic fields are dynamically important. Indeed, much of the turbulence in the interstellar medium is magnetohydrodynamic in nature.

Hydromagnetic turbulence has been explored extensively in connection with the generation of large-scale magnetic fields in astrophysical bodies such as planets, stars, accretion discs, and galaxies through dynamo theories. Nondriven, freely decaying turbulence may also be of interest in connection with both the physics of the interstellar medium and cosmology. Our interest was inspired by the cosmology of primordial magnetic fields, which is sometimes considered as a possible source for providing the seed for the galactic dynamo [1].

There have been various related works on decaying magnetohydrodynamic (MHD) turbulence, by authors interested in different contexts [2–7]. Most directly comparable to our work, Biskamp and Müller [6] studied the energy decay in incompressible three-dimensional (3D) magnetohydrodynamic turbulence in numerical simulations at relatively high Reynolds number, and in a companion letter [7], studied the scaling properties of the energy power spectrum.

We are here especially interested in the inverse cascade of magnetic helicity, whereby magnetic energy is transferred from small-to-large-scale fluctuations. This is important for a primordial magnetic field to reach a large enough scale with sufficient amplitude to be relevant for seeding the galactic dynamo [8].

It should be noted that due to the conformal invariance of MHD in the radiation era, the MHD equations in an expanding universe can be converted into the relativistic MHD equations in flat spacetime by an appropriate scaling of the variables and by using conformal time [9]. The equations of [9] differ slightly from the ordinary nonrelativistic MHD equations. However, in order to facilitate comparison with earlier work, we use the nonrelativistic equations.

We perform 3D simulations both with and without magnetic helicity, starting from statistically homogeneous and isotropic random initial conditions, with power spectra suggested by cosmological applications. We find a strong inverse cascade in the helical case, with equivocal evidence for a weak inverse cascade when only helicity fluctuations are present. In the helical case, we also find a self-similar power spectrum with an approximately $k^{-2.5}$ behavior at high k. We present energy decay laws that are comparable to those found in the incompressible case by Biskamp and Müller [6], and in the compressible case by Mac Low *et al.* [5].

II. THE MODEL

We consider the equations for an isothermal compressible gas with a magnetic field, which is governed by the momentum equation, the continuity equation, and the induction equation, written here in the form

$$\frac{\partial \mathbf{u}}{\partial t} = -\mathbf{u}\cdot\boldsymbol{\nabla}\mathbf{u} - c_s^2\boldsymbol{\nabla}\ln\rho + \frac{\mathbf{J}\times\mathbf{B}}{\rho} + \frac{\mu}{\rho}\left(\nabla^2\mathbf{u} + \frac{1}{3}\boldsymbol{\nabla}\boldsymbol{\nabla}\cdot\mathbf{u}\right), \tag{1}$$

$$\frac{\partial \ln\rho}{\partial t} = -\mathbf{u}\cdot\boldsymbol{\nabla}\ln\rho - \boldsymbol{\nabla}\cdot\mathbf{u}, \tag{2}$$

$$\frac{\partial \mathbf{A}}{\partial t} = \mathbf{u}\times\mathbf{B} + \eta\nabla^2\mathbf{A}, \tag{3}$$

where $\mathbf{B}=\boldsymbol{\nabla}\times\mathbf{A}$ is the magnetic field in terms of the magnetic vector potential $\mathbf{A}$, $\mathbf{u}$ is the velocity, $\mathbf{J}$ is the current density, ρ is the density, μ is the dynamical viscosity, and η is the magnetic diffusivity.

The code for solving these equations [10] uses a variable third-order Runge-Kutta timestep and sixth-order explicit centered derivatives in space. All our runs are performed on a 120^3 grid, and we use periodic boundary conditions, which

*Electronic address: kapl7@pact.cpes.susx.ac.uk
†Electronic address: m.b.hindmarsh@sussex.ac.uk
‡Electronic address: brandenb@nordita.dk

means that the average plasma density $\langle \rho_0 \rangle = \rho_0$ is conserved during runs. Here, ρ_0 is the value of the initially uniform density, and the brackets denote volume average.

We adopt nondimensional quantities by measuring **u** in units of c, where c is the speed of light, **k** in units of k_1, where k_1 is the smallest wave number in the box, which has a size of $L_{\rm BOX}=2\pi$, density in units of $\rho_0=1$, and **B** is measured in units of $\sqrt{\mu_0\rho_0}c$, where μ_0 is the magnetic permeability. This is equivalent to putting $c=k_1=\rho_0=\mu_0=1$. In the following, we will refer to the mean kinematic viscosity ν, which we define as $\nu \equiv \mu/\rho_0$. The sound speed c_s takes the value $c_s=1/\sqrt{3}$, as appropriate for a relativistic fluid. With $c=1$, the unit of time is such that the light crossing time of the box is 2π.

Our equations are similar to those for the relativistic gas in the early universe using scaled variables and conformal time for nonrelativistic bulk velocities [9]. We expect our results to change little using the true relativistic equations, as our advection velocity is at most only mildly relativistic, and this only at the beginning of the simulation.

III. ON THE ROLE OF THE INVERSE CASCADE

The magnetic helicity $H_{\rm M}$ is given by

$$H_{\rm M} = \int \mathbf{A}\cdot\mathbf{B}\, d^3x, \tag{4}$$

and characterizes the linkage between magnetic field lines. $H_{\rm M}$ is conserved in the absence of ohmic dissipation, although it is still possible to have local, small-scale helicity fluctuations. Helicity plays an important role in dynamo theory [11,12], where turbulence is driven.

In many astrophysical and cosmological situations, the magnetic Reynolds number $Re_{\rm M}$ is very large. We define the magnetic Reynolds number as $Re_{\rm M}=Lv/\eta$, where L and v are the typical length scale and velocity of the system under consideration and η is the resistivity. The magnetic Reynolds number is a measure of the relative importance of flux freezing versus resistive diffusion. In a cosmological context, this number can be extraordinarily large: causality imposes the weak limit $L \leqslant ct$ and relativity demands $v<c$. With conductivities relevant to the era when the electroweak phase transition took place [13], one can, in principle, obtain a magnetic Reynolds number of about 10^{16}. This is often taken to mean that the magnetic field is frozen into the plasma, and the scale length of the field increases only with the expansion of the Universe.

However, this simple picture does not necessarily give a full description of the dynamics because the MHD equations, especially at high Reynolds numbers where nonlinear terms are important, exhibit turbulent behavior, which can lead to a redistribution of magnetic energy over different length scales [9]. Energy in a turbulent magnetic field can undergo an inverse cascade and be transferred from high-frequency modes to low-frequency modes, increasing the overall comoving correlation length [11]. This process is due to the nonlinear terms giving rise to interactions between many different length scales.

We will take the initial primordial power spectrum as given and address the question of how such a primordial spectrum evolves as a consequence of the nonlinear equations of motion.

IV. INITIAL CONDITIONS

Since one of the aims of the present work is to investigate the role of magnetic helicity in the inverse cascade, we describe how the initial conditions for our simulations were set up. We chose our initial condition by setting up magnetic fluctuations with an initial power spectrum $P_{\rm M}(k) \equiv \langle \mathbf{B}_{\mathbf{k}}^* \cdot \mathbf{B}_{\mathbf{k}} \rangle \approx k^n$ in Fourier space (and averaged over shells of constant $k=|\mathbf{k}|$), for low values of the wave-number k, using an exponential cutoff k_c. [The shell-averaged power spectrum $P_{\rm M}(k)$ is not to be confused with the shell-integrated energy spectrum, $E_{\rm M}=4\pi k^2 \times (1/2) P_{\rm M}(k)$, which is shown in the plots below.]

The magnetic-field fluctuations are drawn from a Gaussian random-field distribution fully determined by its power spectrum in Fourier space according to the following procedure. For each grid point, we use the corresponding wave number to select an amplitude from a Gaussian distribution centered on zero and with the width

$$P_{\rm M}(k) = P_{\rm M,0} k^n \exp[-(k/k_c)^4], \tag{5}$$

where $k=|\mathbf{k}|$. We then transform the field back into real space to obtain the field at each grid point. This is done independently for each field component.

There is a requirement in cosmology that $n \geqslant 2$, which is set by causality demanding that the correlation function of the magnetic field vanishes at large distances, and the fact that the magnetic field is divergence-free [14]. In the simulations presented, we chose the slope of the power spectrum to be $n=2$. We also chose $k_c=30$, unless specified otherwise, which gives a power spectrum peaked at a relatively large value of k. Biskamp and Müller [6,7] started with a spectrum peaked at $k_c=4$, which may account for the different slope in the late-time power spectrum that we observe (see Sec. V A).

Our velocity power spectrum was chosen in a similar way, but with $n=0$ corresponding to white noise at large scales (there is no requirement for incompressibility in the early universe). The initial magnetic energy was taken equal to the kinetic energy, and had the value 5×10^{-3} in all runs, as the primordial field is thought likely to be weak.

In order to introduce a nonzero average magnetic helicity into the system, it is useful to represent the vector potential in terms of its projection onto an orthogonal basis formed by $\hat{\mathbf{e}}_+$, $\hat{\mathbf{e}}_-$, and $\hat{\mathbf{k}}$. The two basis vectors $\hat{\mathbf{e}}_+$ and $\hat{\mathbf{e}}_-$ can be chosen to be the unit vectors for circular polarization, right-handed and left-handed, respectively. That is, $\hat{\mathbf{e}}_\pm = \hat{\mathbf{e}}_1 \pm i\hat{\mathbf{e}}_2$, where $\hat{\mathbf{e}}_1$ and $\hat{\mathbf{e}}_2$ are unit vectors orthogonal to each other and to **k**. They are given by $\hat{\mathbf{e}}_1 = \mathbf{k}\times\hat{\mathbf{z}}/|\mathbf{k}\times\hat{\mathbf{z}}|$ and $\hat{\mathbf{e}}_2 = \mathbf{k}\times(\mathbf{k}\times\hat{\mathbf{z}})/|\mathbf{k}\times(\mathbf{k}\times\hat{\mathbf{z}})\hat{\mathbf{z}}|$, respectively. $\hat{\mathbf{z}}$ is a reference direction.

Note that since

$$i\hat{\mathbf{k}}\times\hat{\mathbf{e}}_s = sk\hat{\mathbf{e}}_s, \tag{6}$$

where $s=\pm 1$, this corresponds to an expansion of the magnetic vector potential into helical modes.

Using these basis vectors, it is easily seen that the magnetic energy spectrum is

$$E_{\mathrm{M}}(k) = 2\pi k^2 \langle |\mathbf{B}_{\mathbf{k}}|^2 \rangle, \tag{7}$$

where the amplitude of the magnetic field is given by

$$|\mathbf{B}_{\mathbf{k}}|^2 = (|A_{\mathbf{k}}^+|^2 + |A_{\mathbf{k}}^-|^2)|\mathbf{k}|^2 \tag{8}$$

and the expression for the magnetic helicity spectrum $H_{\mathrm{M}}(k)$ is

$$H_{\mathrm{M}}(k) = 4\pi k^2 \langle \mathbf{A}_{\mathbf{k}}^* \cdot \mathbf{B}_{\mathbf{k}} \rangle, \tag{9}$$

where

$$\mathbf{A}_{\mathbf{k}}^* \cdot \mathbf{B}_{\mathbf{k}} = (|A_{\mathbf{k}}^+|^2 - |A_{\mathbf{k}}^-|^2)|\mathbf{k}|. \tag{10}$$

The function $H_{\mathrm{M}}(k)$ is a sensitive measure of the correlation between the vector potential and the magnetic field. $H_{\mathrm{M}}(k)$ may, of course, be positive in one part of Fourier space and negative in another part. It is, however, bounded in magnitude by the inequality

$$|H_{\mathrm{M}}(k)| \leqslant 2k^{-1} E_{\mathrm{M}}(k). \tag{11}$$

A field that saturates the above inequality is maximally helical.

The amplitudes $A_{\mathbf{k}}^{\pm}$ can be chosen independently, provided $A_{-\mathbf{k}}^{*\pm} = A_{\mathbf{k}}^{\pm}$, which is just the condition that the vector potential be real. Therefore, it is possible to adjust the amplitudes $|A_{\mathbf{k}}^+|$ and $|A_{\mathbf{k}}^-|$ freely and in so doing obtaining a magnetic field with arbitrary magnetic helicity. With our method, we are able to put statistically random but maximally helical fields in our initial conditions. In our runs with initial helicity, we take $H_{\mathrm{M}} = H_{\max}$.

Because we evolve our dynamical fields on a discrete lattice we have to be careful when using derivative operations in Fourier space. In general, the wave vector, which is an eigenvalue of the derivative operator, needs to be replaced by some function $k_{\mathrm{eff}}(k)$, which is an eigenvalue of the discrete derivative operator on the lattice. In our case, we have for the sixth-order explicit centered derivative

$$k_{\mathrm{eff}}(k) = \frac{1}{30}[\sin(3k) - 9\sin(2k) + 45\sin(k)]. \tag{12}$$

In order to be consistent with the scheme used in the simulation, we use $k_{\mathrm{eff}}(k)$ when calculating the initial condition in Fourier space.

V. RESULTS

In all runs, the mean kinematic viscosity ν and the resistivity η were chosen to be equal with values between $\nu = \eta = 5\times 10^{-4} - 5\times 10^{-5}$. In our simulations, we typically obtain Reynolds numbers of the order of 100–200. The Reynolds numbers in our simulations are evaluated using the magnetic Taylor microscale, which we calculate here as the ratio of the rms magnetic field and the rms current density, $L_{\mathrm{T}} = 2\pi B_{\mathrm{rms}}/J_{\mathrm{rms}}$. The 2π factor is here included so that L_{T} represents the typical wavelength (and not the inverse wave number) of structures in the current density.

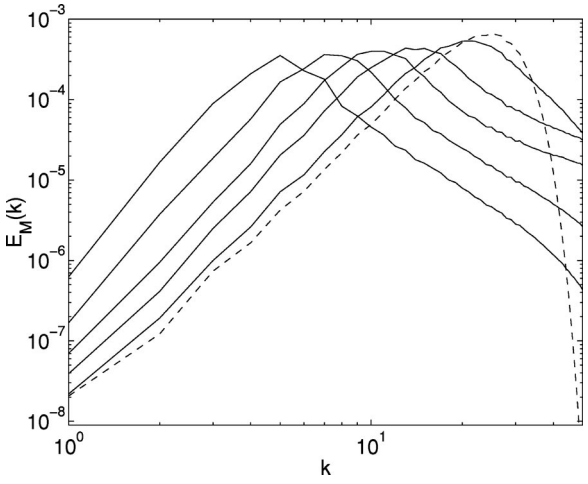

FIG. 1. Magnetic energy spectrum $E_{\mathrm{M}}(k)$ for a run with finite magnetic helicity, $\nu = \eta = 5\times 10^{-5}$. The times shown are 0, 1.0, 4.6, 10.0, 21.5, and 46.3. The initial spectrum is indicated by the dashed line. At low wavenumbers k, the energy spectrum $E_{\mathrm{M}}(k)$ increases with time.

A. Spectral evolution

The inverse magnetic cascade for decaying MHD turbulence is best visualized in terms of magnetic energy spectra $E_{\mathrm{M}}(k)$ because information on nonlinear interaction between different scales is contained in $E_{\mathrm{M}}(k)$. In Fig. 1, we show a run with initial magnetic helicity. In Fig. 1, we see evidence for a dual energy transfer both toward higher and lower wave numbers. The inverse cascade is characterized by the transfer of energy from small-scale structures in the magnetic field to larger ones. In Fig. 1, this behavior is clearly seen as indicated by the rise in the energy spectrum at small wave numbers. Some energy is also being transported to smaller scales where the spectrum is decaying due to diffusive effects. We also note that at wave numbers above the peak $k_p(t)$, the spectrum develops a power-law shape. This power law has approximately a $k^{-2.5}$ slope. This differs from the approximately $k^{-5/3}$ law found by Müller and Biskamp [7]. We suggest that this is due to finite-size effects, which affect the spectrum if the initial scale separation between k_p and the smallest wave number in the box ($k=1$) is insufficient, and if the flow is strongly helical so that its spectrum is governed by inverse cascading. In order to check this, we have performed a run with larger initial length scale, $k_c = 5$. In this case, the magnetic energy spectrum develops into an approximate $k^{-5/3}$ law at late times. However, this occurs only after the peak of the spectrum has left the simulation box, i.e., after finite-size effects have begun to play a role.

To check if the magnetic-field evolution is self similar, one can make the following ansatz for the energy spectrum

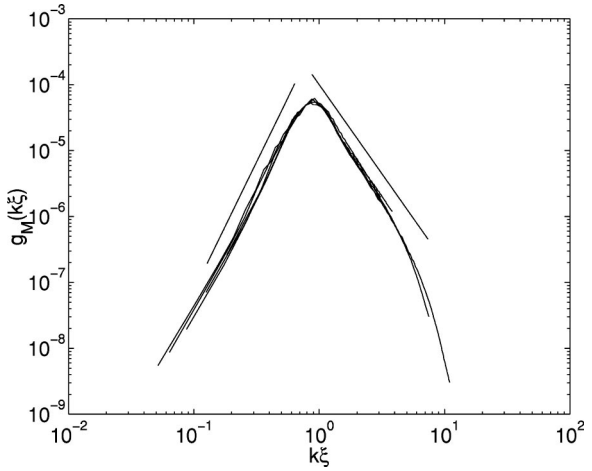

FIG. 2. The magnetic scaling function $g_M(k\xi)$ described in the text, Eq. (13), versus $k\xi$. The straight lines indicate the power laws $\propto(k\xi)^{4.0}$ and $\propto(k\xi)^{-2.5}$, respectively.

$$E_M(k,t)=\xi(t)^{-q}g_M(k\xi). \tag{13}$$

Here, ξ is the characteristic length scale of the magnetic field, taken to be the magnetic Taylor microscale defined above, and q is a parameter whose value is some real number. We call $g_M(k\xi)$ the magnetic scaling function. In Fig. 2, we have plotted $\xi(t)^q E_M(k,t)$ versus the scaled variable $k\xi(t)$. The value of the parameter q in this run is $q=0.7$. It is seen that for each different value of time t, the data collapses onto a single curve given by the scaling function $g_M(k\xi)$, demonstrating the self similarity of the magnetic field evolution.

We also performed runs in which the magnetic helicity was zero, in the statistical sense. Magnetic helicity was present due to fluctuations, but was of very small amplitude. In these runs, no significant inverse cascade was observed. Figure 3 shows the energy spectrum for such a run with only

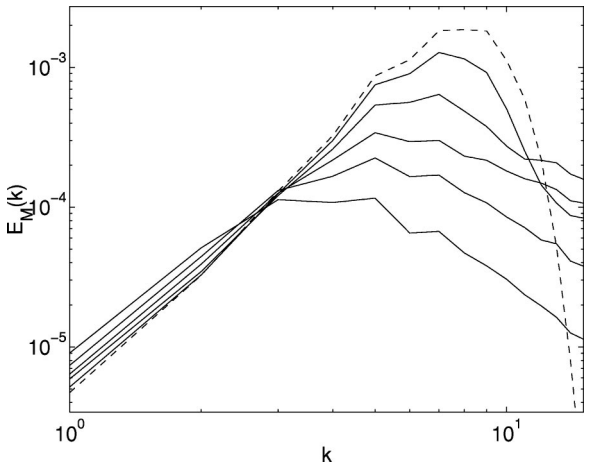

FIG. 3. Magnetic energy spectrum $E_M(k)$ for a run with no net magnetic helicity. $\nu=\eta=1\times10^{-4}$. Here, $k_c=10$. The times shown are 0, 2.2, 4.6, 10.0, 21.5, and 46.3. The initial spectrum is indicated by the dashed line. The peak of the energy spectrum $E_M(k)$ is decreasing with increasing time.

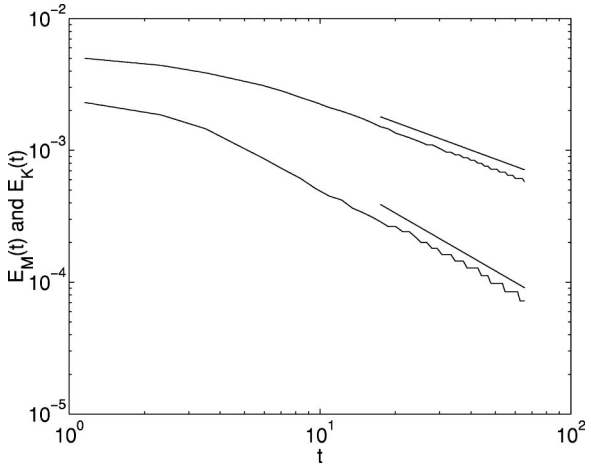

FIG. 4. Time evolution of the magnetic energy $E_M(t)$ and the kinetic energy $E_K(t)$ in the case where there is initial magnetic helicity. $\nu=\eta=5\times10^{-5}$. The straight lines indicate the power laws $\propto t^{-0.7}$ and $\propto t^{-1.1}$, respectively.

small magnetic helicity fluctuations present in the initial conditions. It is seen that only a weak inverse cascade is present at the lowest wave numbers, much smaller than in the helical case. However, that it seems to be present at all is interesting as the effect could become more pronounced for higher Reynolds numbers. It is possible that this effect is due to the magnetic helicity fluctuations even though they were small. One simulation was performed with identically zero initial magnetic helicity fluctuations. In this case, random fluctuations develop rapidly and no differences between the two cases were observed.

B. Energy decay

In Fig. 4, we show the time evolution of the magnetic energy $E_M(t)$ and the kinetic-energy $E_K(t)$ for a run with initial helicity and a k^4 initial energy spectrum slope. It is seen that the asymptotic decay rate for $E_M(t)$ is approximately $t^{-0.7}$. The Reynolds number for this run was around $Re\sim200$ at late times. In another run with $Re\sim100$, the decay rate was seen to be $t^{-0.8}$, so there seems to be a dependence of the decay rate of the magnetic field on the Reynolds number and perhaps the resulting slope of the spectrum.

The kinetic energy also decays with a power-law behavior at late times. In the case of runs with initial helicity, the kinetic-energy $E_K(t)$ decays with a different, faster rate than $E_M(t)$. The asymptotic decay rate is close to $t^{-1.1}$. In runs without initial helicity, the decay rates of $E_M(t)$ and $E_K(t)$ are approximately the same, close to $t^{-1.1}$.

In our runs with $E_K=E_M$ initially, the kinetic-energy spectrum shows no evidence of an inverse cascade at any scale. However, when the initial velocity distribution is zero, the kinetic spectrum grows on all scales initially and in the low wave-number region, the energy continues to grow even after the high wave-number modes start to decay.

C. Coherence length evolution

During the course of the simulations, the initially small-scale structures gain in size. A convenient length scale is the

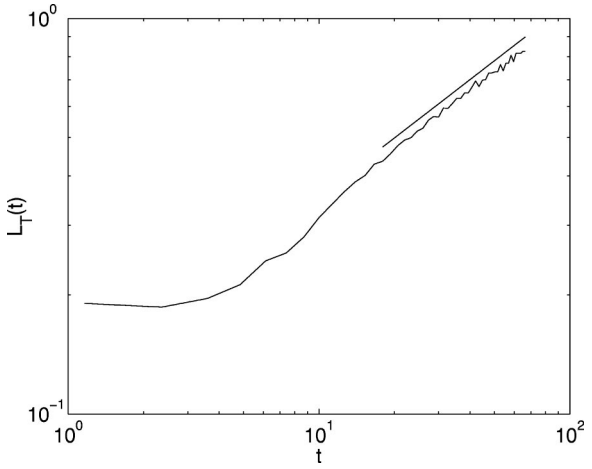

FIG. 5. Time evolution of the magnetic Taylor microscale for the case with initial magnetic helicity. $\nu=\eta=5\times10^{-5}$. The straight line indicates the power law $\propto t^{0.5}$.

magnetic Taylor microscale L_{T}, which was defined above. This length scale is mostly characteristic of the small scales but even they grow during the course of the simulations.

In Fig. 5, we show the evolution of L_{T} for a run with initial helicity. The asymptotic behavior of the length scale is seen to grow approximately as $L_{\mathrm{T}}\sim t^{0.5}$.

In runs with nonhelical initial conditions, the growth of the magnetic Taylor microscale is slower than in the case of helical initial conditions. In this case, the magnetic Taylor microscale grows approximately as $L_{\mathrm{T}}\sim t^{0.4}$.

The discussion so far has mainly been concerned with the evolution of causally generated magnetic fields using an initial k^4 slope in the magnetic energy spectrum. Now we briefly comment on the other cases we have looked at. For a white-noise initial spectrum $E_{\mathrm{M}}(k)\sim k^2$, the evolution is qualitatively and quantitatively similar to the causal case. For helical fields, we observe an inverse cascade, while for nonhelical fields, a much smaller inverse cascade is present only for the lowest modes.

VI. DISCUSSION

Our simulations show the decay rate of magnetic energy for compressible turbulence being sensitive to the initial helicity of the magnetic field configuration. A similar result was found in [6] in the case of incompressible turbulence. The fact that magnetic helicity is conserved (except for resistive changes), and the magnetic energy decays slower for helical fields, is connected with the observed inverse cascade in which magnetic energy is transported toward larger scales because of nonlinear dynamics.

The decay of kinetic energy does not seem to depend on the initial helicity and its decay rate $E_K(t)\sim t^{-1.1}$ is consistent with the earlier work of [5,6]. Note that in the helical case, we observe the kinetic energy decaying more rapidly than the magnetic one; this behavior was also found in [6].

While these results are not directly applicable to the evolution of primordial magnetic fields in the early universe, they do suggest that nonlinear magnetohydrodynamical effects may play an important role in this case.

In any case, it is interesting to compare our results with the work of other authors interested in the decay properties of cosmological magnetic fields [15–18]. Ideal MHD has a scale invariance that leads to the scaling law [15,17]

$$E_M(t,k)=k^{-1-2h}\psi(k^{1-h}t), \tag{14}$$

where ψ is an unknown function, related to g_{M}. Assuming it is peaked somewhere, and $h<0$, the characteristic scale of the field goes as $L(t)\sim t^{1/(1-h)}$. It is also often assumed that $\psi(0)$ exists and is nonzero: thus, h is determined by the initial power spectrum. Hence, for a magnetic power spectrum of index n, $h=-(n+3)/2$ and

$$L(t)\sim t^{2/(n+5)}. \tag{15}$$

This law may also be recovered by assuming that the characteristic time scale for the decay of turbulence on a scale l is the eddy turnover time $\tau_l=l/v_l$, where $v_l\sim l^{-(n+3)}$ is the velocity averaged on a scale l [16]. If the characteristic scale of the field is that scale that is just decaying, then $\tau_L\sim t$, and we again find Eq. (15). One should note that these arguments ignore helicity conservation.

We recall that our nonhelical runs had $n=2$ for the magnetic power spectrum and $n=0$ for the velocity power spectrum. The observed growth law for the magnetic Taylor microscale $t^{0.4}$ is not consistent with the predicted power law for $n=2$, although it does square with the growth law for $n=0$, and it is possible that the growth in the magnetic field length scale is being controlled by the velocity field. Simulations at higher Reynolds numbers seem required to resolve this issue.

One would expect on integrating the helicity power spectrum that $H_M\sim L_I E_M$, where L_I is the integral scale. We would expect that $L_I\sim L_T$, and hence, if magnetic helicity is conserved,

$$E_M\sim L_T^{-1}. \tag{16}$$

However, magnetic helicity is not conserved exactly: we observe a decrease in H_{M} by a factor of about two in a run with viscosity $\nu=5\times10^{-5}$. Indeed, with $L_T\sim t^{0.5}$ we find a somewhat steeper relation: $E_M\sim t^{-0.7}\sim L_T^{-1.4}$.

Finally, it is interesting to note that Son's numerical simulations of decaying turbulence [16], performed in the eddy-damped quasinormal Markovian (EDQNM) approximation, show some evidence of a power law developing at high k, the slope being close to $k^{-2.5}$, although there was no net helicity present, and no inverse cascade. Furthermore, Field and Carroll [18], again using the EDQNM approximation, found that there were self-similar solutions with $E_M\sim t^{-2/3}\sim L_T^{-1}$.

VII. CONCLUSIONS

We have shown that for an isothermal and compressible magnetized turbulent fluid, when undergoing a process of free decay, a substantial inverse cascade is present for helical magnetic field configurations, which transfer energy from

smaller-scale magnetic fluctuation to larger-scale ones. For nonhelical magnetic fields, only a weak inverse cascade was observed on the largest scales.

The energy spectrum of the magnetic field shows evidence for a self-similar evolution with a development of a power law of roughly $k^{-2.5}$ beyond the peak. Decay laws for both the kinematic and magnetic energy were found. The kinetic-energy decay was approximately $t^{-1.1}$ for both helical and nonhelical magnetic fields. The decay of the magnetic field energy was found to be strongly dependent on the the initial helicity, decaying roughly as $t^{-0.7}$ and $t^{-1.1}$ for helical and nonhelical initial conditions, respectively. For the helical case, the magnetic energy decay rate showed a dependence on the Reynolds number, with a slower decay rate for larger Reynolds numbers.

We also observed power-law behavior in the characteristic length scale of the magnetic field, defined as the Taylor microscale L_T. In the helical case $L_T \sim t^{0.5}$, whereas for nonhelical fields the growth was somewhat slower, $L_T \sim t^{0.4}$, and we ascribe the faster growth rate to the presence of the inverse cascade in the helical case.

ACKNOWLEDGMENTS

This work was conducted on the Cray T3E and SGI Origin platforms using COSMOS Consortium facilities, funded by HEFCE, PPARC, and SGI. We also acknowledge computing support from the Sussex High Performance Computing Initiative.

[1] Ya.B. Zeldovich, A.A. Ruzmaikin, and D.D. Sokoloff, *Magnetic Fields in Astrophysics* (Gordon and Breach, New York, 1983); A.A. Ruzmaikin, A.A. Shukurov, and D.D. Sokoloff, *Magnetic Fields in Galaxies* (Kluwer, Dordrecht, 1988).

[2] M. Hossain, P. Gray, D. Pontius, W. Matthaeus, and S. Oughton, Phys. Fluids **7**, 2886 (1995).

[3] H. Politano, A. Pouquet, and P.L. Sulem, in *Small-Scale Structures in Fluids and MHD*, edited by M. Meneguzzi, A. Pouquet, and P.L. Sulem, Springer-Verlag Lecture Notes in Physics Vol. 462 (Springer-Verlag, Berlin, 1995), p. 281.

[4] S. Galtier, H. Politano, and A. Pouquet, Phys. Rev. Lett. **79**, 2807 (1997).

[5] M. Mac Low, R.S. Klessen, A. Burkert, and M.D. Smith, Phys. Rev. Lett. **80**, 2754 (1998).

[6] D. Biskamp and W.C. Müller, Phys. Rev. Lett. **83**, 2195 (1999).

[7] W.C. Müller and D. Biskamp, Phys. Rev. Lett. **84**, 475 (2000).

[8] M. Hindmarsh and A. Everett, Phys. Rev. D **58**, 103 505 (1998).

[9] A. Brandenburg, K. Enqvist, and P. Olesen, Phys. Rev. D **54**, 1291 (1996).

[10] A. Brandenburg, Astrophys. J. **550**, 824 (2001).

[11] A. Pouquet, U. Frisch, and J. Leorat, J. Fluid Mech. **77**, 321 (1976).

[12] M. Meneguzzi, U. Frisch, and A. Pouquet, Phys. Rev. Lett. **47**, 1060 (1981).

[13] J. Ahonen and K. Enqvist, Phys. Lett. B **382**, 40 (1996).

[14] R. Durrer, T. Kahniasvili, and A. Yates, Phys. Rev. D **58**, 123 004 (1998).

[15] P. Olesen, Phys. Lett. B **398**, 321 (1997).

[16] D.T. Son, Phys. Rev. D **59**, 063 008 (1999).

[17] T. Shiromizu, Phys. Lett. B **443**, 127 (1998).

[18] G.B. Field and S.M. Carroll, Phys. Rev. D **62**, 103008 (2000).